RSC Sustainability

ROYAL SOCIETY OF CHEMISTRY

PAPER

View Article Online
View Journal | View Issue

Cite this: *RSC Sustainability*, 2026, **4**, 1485

Sustainable bio-based isocyanate-free poly (urethane amic acid) coatings for the corrosion protection of mild steel

Rakesh Rapolu,†[a] Kashmiri Borah, †[ab] P. Ermiya Prasad,[ab] Aqueeb Javeed[a] and Aruna Palanisamy *[ab]

In pursuit of sustainable and environmentally benign coating technologies, we report the synthesis and evaluation of isocyanate-free/non-isocyanate poly (urethane amic acid) (NIPUAA) coatings developed from a renewable source, castor oil. NIPUAA was prepared using a step-growth polymerization strategy using functionalized castor oil (carbonated castor oil, CCO), isophorone diamine and pyromellitic dianhydride, eliminating the need for toxic isocyanates. The chemical structure of the synthesized NIPUAA was confirmed by FTIR and NMR spectroscopy, indicating the successful formation of urethane and amic acid linkages. The thermal transitions and stability were analyzed using DSC and TGA. The results showed a moderate level of thermal endurance, suitable for coating applications. The NIPUAA coatings were coated on mild steel substrates and subjected to a thorough performance evaluation, including Tafel polarisation, electrochemical impedance spectroscopy (EIS), and salt spray testing for corrosion resistance. Pencil hardness, abrasion resistance, adhesion test, and cone mandrel flexibility tests were used to assess mechanical durability. The coatings demonstrated competitive performance in comparison to conventional systems, with satisfactory corrosion inhibition and mechanical integrity. These findings demonstrate the potential of NIPUAA derived from castor oil as a promising candidate for isocyanate-free protective coatings, providing a more environmentally friendly option for multipurpose metal surface protection.

Received 31st October 2025
Accepted 21st January 2026

DOI: 10.1039/d5su00835b

rsc.li/rscsus

Sustainability spotlight

This work advances sustainable coating technology by developing an isocyanate-free poly (urethane amic acid) (NIPUAA) derived from renewable castor oil, thereby eliminating the use of toxic isocyanates and reducing petrochemical dependency. The synthesis employs a greener, step-growth polymerization approach using bio-based reactants and solvent-free processing. The resulting coatings exhibit strong corrosion resistance and mechanical performance, validating their suitability as eco-friendly alternatives to conventional polyurethane coatings. This research directly supports the United Nations Sustainable Development Goals (SDGs), particularly SDG 12 (Responsible Consumption and Production) and SDG 13 (Climate Action), by promoting sustainable material innovation, safer chemical processes, and the utilization of renewable resources for a cleaner, more sustainable industrial future.

1. Introduction

Significant innovation in the development of more environmentally friendly and sustainable polymer systems has gained momentum in recent decades due to the increased focus on sustainability, environmental safety, and occupational health. Traditionally valued for their excellent adhesion, flexibility, abrasion resistance, and chemical durability, polyurethane coatings are used extensively in a variety of industries, including marine,[1] automotive,[2] aerospace,[3] and construction,[4] to prevent corrosion and to achieve mechanical durability and surface aesthetics. However, diisocyanates, a class of extremely toxic and reactive substances derived from phosgene chemistry, are used in the synthesis of conventional polyurethanes.[5] Diisocyanates, like methylene diphenyl diisocyanate (MDI) and toluene diisocyanate (TDI), present serious risks to human health and the environment, including the potential risk for cancer, dermal toxicity, and respiratory sensitisation.[6,7] This makes handling and processing them more difficult and raises questions about their long-term ecological impact and compliance with international regulations. Consequently, the development of non-isocyanate polyurethane (NIPU) analogues has emerged as a key research direction in the quest for greener and more sustainable coating technologies.[8–10] In this context, non-isocyanate poly (urethane

[a]*Polymers and Functional Materials Department, CSIR-Indian Institute of Chemical Technology (CSIR-IICT), Hyderabad 500007, India. E-mail: aruna.iict@csir.res.in; aruna@csiriict.in*

[b]*Academy of Scientific and Innovative Research (AcSIR), Ghaziabad 201002, India*

† R. R. and K. B. contributed equally to the manuscript.

amic acids) (NIPUAAs) have emerged as a promising class of polymers. Although there have been a few reports on poly (urethane amic acids) (PUAA), literature related to the synthesis of non-isocyanate poly (urethane amic acids) (NIPUAAs) has been quite rare.[11,12] Although these materials share structural similarities with conventional polyurethanes, they are prepared without the use of isocyanates by reacting hydroxyl-functionalized polyols with diamines and dianhydrides. While the urethane linkage ensures flexibility and thermal stability, the amic acid moiety offers numerous hydrogen-bonding sites, enhancing cohesive strength and adhesion potential. Despite these advantages, there are still very few reports on PUAA-based coatings, particularly regarding formulations made from renewable feedstocks.[13]

Furthermore, high-performance coatings that incorporate bio-based polyols align well with the circular materials economy and green chemistry principles. Among the available natural polyols, castor oil stands out because of its distinct molecular structure. About 90% of it is ricinoleic acid, which provides a mixture of unsaturated, carboxylic, and hydroxyl groups suitable for direct functionalisation. It is a very desirable raw material for polymer synthesis due to its availability, cost-effectiveness, chemical stability, and biodegradability. Castor oil can function as an effective building block for non-isocyanate poly (urethane amic acid) (NIPUAA) systems when chemically modified to add reactive hydroxyl groups suitably. Recent studies have explored the synthesis of castor oil-based NIPUs, with promising results for both mechanical performance and corrosion prevention. Castor oil-based coatings, for example, have demonstrated positive outcomes in terms of adhesion, hardness, and resistance to corrosive environments.[14,15] Nevertheless, there have been few thorough analyses that take into account mechanical, thermal, and electrochemical characteristics, which calls for more studies in this area. Building on this bio-based vision, it becomes equally crucial to address the performance challenges posed by conventional materials in real-world environments. Despite being one of the most popular structural materials because of its exceptional strength-to-cost ratio, mild steel is highly prone to corrosion, especially in harsh industrial, acidic, and marine environments.[16] Corrosion not only undermines structural integrity but also imposes heavy economic burdens, accounting for more than 3% of the global GDP annually.[17] The conventional solution has been to apply protective coatings, especially polyurethanes, which serve as chemical and physical barriers against corrosive ions, oxygen, and moisture. However, these systems often employ hazardous isocyanate-based chemicals, which raises significant concerns regarding their environmental and human health safety. This has prompted an urgent shift toward greener, safer alternatives. Thus, integrating bio-derived castor oil with NIPUAA chemistry holds the potential not only to meet but to redefine performance expectations for protective coatings, blending sustainability with superior protection. However, achieving both corrosion resistance and mechanical durability using a green, non-toxic, and bio-based polymeric system remains an important yet challenging objective. Herein, we report the synthesis of a bio-based non-isocyanate poly(urethane amic acid) (NIPUAA) coating system using carbonated castor oil (CCO) derived from epoxidized castor oil and CO_2. Ring opening of the 5-membered cyclic carbonate ring with isophorone diamine (IPDA) and chain extension with pyromellitic dianhydride (PMDA) yielded the desired NIPUAA. Variations with respect to the CCO : IPDA : PMDA mole ratio of 1 : 2 : 1, 1 : 3 : 2 and 1 : 4 : 3 were carried out to attain the optimum performance of the resulting coatings.

2. Experimental section

2.1 Materials

Castor oil (CO) [hydroxy number (OH) = 170 mg KOH g^{-1}; acid value = 1.27 mg KOH g^{-1}] was purchased from Alfa Aesar.

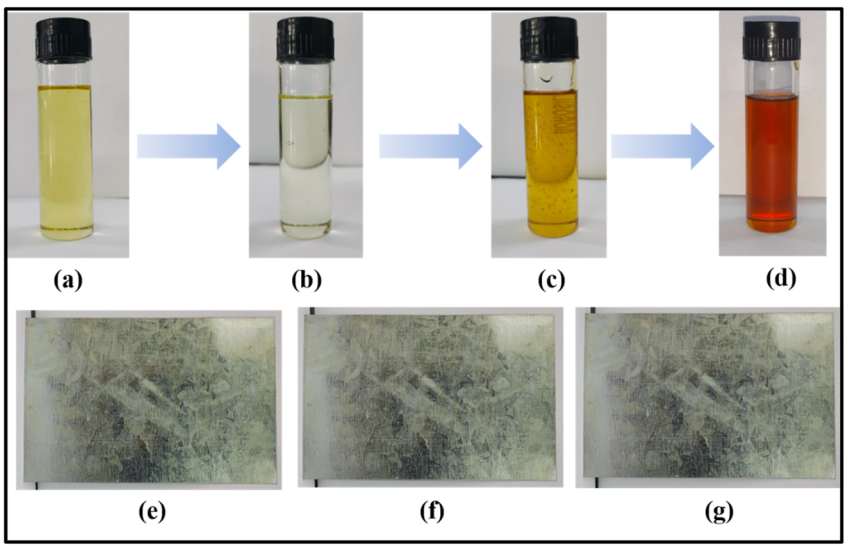

Fig. 1 Appearance of: (a) castor oil (CO), (b) epoxidised castor oil (ECO), (c) carbonated castor oil (CCO), (d) NIPUAA and the plates coated with (e) NIPUAA-121, (f) NIPUAA-132, and (g) NIPUAA-143.

Hydrogen peroxide (H_2O_2, 30% v/v) and stannous octoate (KOSMOS) were purchased from SD Fine Chemicals Limited, India. Anhydrous glacial acetic acid, sodium carbonate (Na_2CO_3), sodium bicarbonate ($NaHCO_3$), and sodium chloride (NaCl) were obtained from Finar Chemicals. Seralite SRC-120 was obtained from Sisco Research Laboratories, India. Tetrabutylammonium bromide (TBAB), triethylamine (Et_3N), diethyl ether, magnesium sulfate anhydrous ($MgSO_4$), and dimethylformamide (DMF) were obtained from AVRA chemicals. Pyromellitic dianhydride (PMDA) and isophorone diamine (IPDA) were purchased from Sigma-Aldrich. All the above chemicals were used as received.

2.2 Methods

2.2.1 Synthesis of epoxidized castor oil (ECO) and carbonated castor oil (CCO). ECO [Fig. 1(b)] and CCO [Fig. 1(c)] were prepared as per previously reported procedures [18,19] from castor oil (CO) [Fig. 1(a)] as shown in Scheme 1. The physicochemical properties of CO [Table S1], ECO [Table S2], and CCO [Table S3] have been provided in Section S1 of SI.

2.2.2 Synthesis of non-isocyanate poly (urethane amic acid) (NIPUAA). A clean, dry, 500 ml, 2-neck, round-bottom flask equipped with a mechanical stirrer was charged with CCO (40 g, 0.035 mol) and IPDA (12.1 g, 0.071 mol). 2–3 drops of diluted KOSMOS (1% in toluene) catalyst were added to the flask, and the reaction mixture was stirred for 8 h at 80 °C. After 8 h, DMF was added to the reaction mixture while maintaining the temperature at 80 °C. The reaction mixture was then allowed to cool gradually to room temperature, and finally, PMDA (7.7 g, 0.035 mol) was added to the cooled mixture. The resulting solution was stirred thoroughly and allowed to react overnight under ambient conditions to give the final NIPUAA polymer, a dark brown viscous oil [Fig. 1(d)], as shown in Scheme 1.

2.2.3 Preparation of coated plates. The NIPUAA reaction mixture was applied to mild steel and galvanized iron (GI) (6 cm × 4 cm) sheets using a brush and was allowed to cure at room temperature for 24 h to obtain a uniform coating of 100 microns thickness.

2.3 Analytical characterization

2.3.1 Proton nuclear magnetic resonance (^{1}H-NMR) spectroscopy. The ^{1}H-NMR spectra were recorded in a Bruker Avance-400 MHz spectrometer instrument using deuterated chloroform ($CDCl_3$) as the solvent at room temperature. The chemical shifts are shown relative to tetramethylsilane (TMS) as the reference standard and expressed in parts per million (ppm).

2.3.2 Fourier transform-infrared (FT-IR) spectroscopy. FT-IR spectra of CO, ECO, CCO and cured NIPUAA free-standing films were measured using a PerkinElmer spectrophotometer (Spectrum 100) within the frequency range of 4000–400 cm^{-1}. The transmittance graphs were observed using KBr pellets.

2.3.3 Thermogravimetric analysis (TGA). TGA analysis was performed using a TA Q500 thermogravimetric analyzer (TA Instruments, New Castle, DE, USA) under a nitrogen atmosphere. A sample weighing 5–10 mg was heated from room temperature to 600 °C at 10 °C min^{-1}.

2.3.4 Differential scanning calorimetry (DSC). DSC curves of the NIPUAA films were recorded in a DSC-Q-100 model of the TA instrument. The samples (approximately 8–10 mg each) were heated at a rate of 10 °C min^{-1} under nitrogen from −70 °C to 220 °C to determine the glass transition temperature. Each run was performed by first heating the sample from room temperature to 150 °C, cooling it to −70 °C and then reheating it to 220 °C.

2.3.5 Adhesion strength. In accordance with ASTM D-4541, the adhesion strength of NIPUAA coatings on mild steel was assessed using an automatic adhesion pull-off tester (PosiTest AT-A, Automatic adhesion tester) for a thickness range of 100 microns.

2.3.6 Abrasion resistance. CS-10 wheels were utilised for 1000 cycles, and abrasion resistance was measured in terms of weight loss (mg) using the Taber abrasion tester (USA) in accordance with ASTM-D4060 standards.

2.3.7 Pencil hardness. Using Mitsubishi pencils with hardness levels ranging from 6B to 6H, the pencil hardness tester (SIIN 501, Samriddhi International Private Limited, India) was used to assess the hardness of the cured NIPUAA coatings on mild steel in accordance with ASTM D3363 standards.

2.3.8 Cone mandrel. The cone mandrel flexibility test of the NIPUAA coating applied to mild steel was evaluated using a flexibility tester (SbS Testing Studio) according to ASTM D522 standards.

2.3.9 Electrochemical studies. Tafel potentiodynamic polarization and electrochemical impedance spectroscopy (EIS) were conducted using a Metrohm Autolab electrochemical workstation (Potentiostat/Galvanostat, Model 302N) operated with NOVA 1.11 software (Metrohm B.·V., Netherlands). Tafel polarization curves were obtained within a potential window of ±200 mV relative to the open circuit potential (OCP), at a scan rate of 5 mV s^{-1}. For EIS measurements, a sinusoidal voltage perturbation of 10 mV was applied across a frequency range from 10^5 to 10^{-2} Hz.

2.3.10 Salt spray test. The corrosion resistance of the coated mild steel (MS) panels was evaluated using the ASTM B-117 salt spray fog test (Komal Scientific Pvt. Ltd, Mumbai, India). Before testing, cross-cuts were introduced on the coated surface to assess the protective efficacy of the coating. The panels were then placed in a salt spray chamber and exposed to a 5% (w/v) NaCl solution for 120 hours under controlled conditions.

3. Results and discussion

Bio-based NIPUAA coatings were strategically designed to assess their applicability as sustainable, isocyanate-free protective films. Their molecular architecture integrates both flexibility and rigidity, enabling a balanced profile in terms of structure-property, adhesion, abrasion resistance, surface hardness, and mechanical flexibility, which are the key parameters relevant to corrosion-resistant coating systems.

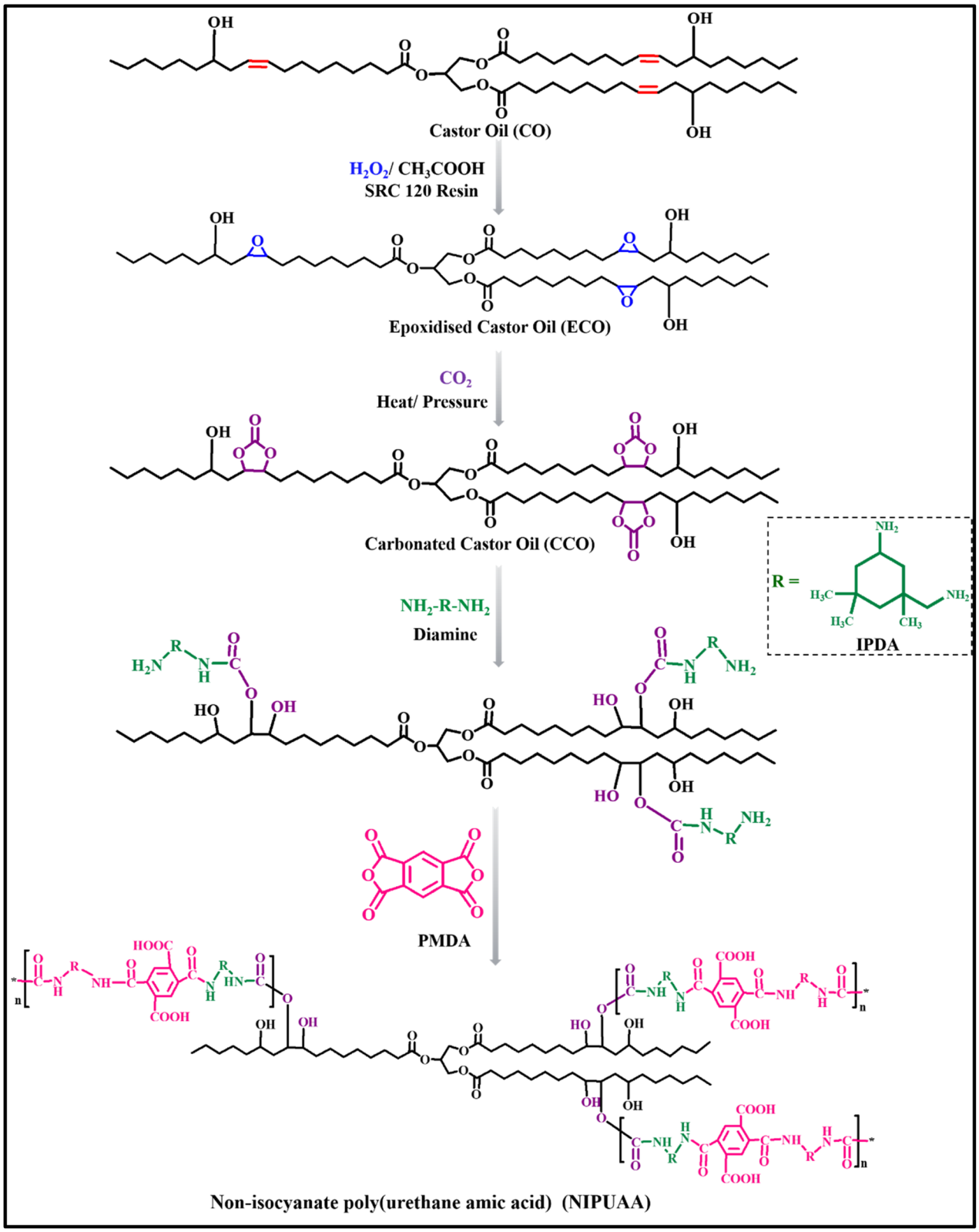

Scheme 1 Synthetic route for the preparation of the NIPUAA polymer from castor oil (CO), a renewable source.

3.1 Structural confirmation

3.1.1 ^{1}H-NMR spectroscopy. As shown in Fig. 2, proton nuclear magnetic resonance (^{1}H-NMR) spectroscopy was employed to monitor and confirm the progressive chemical transformation from castor oil (CO) to epoxidized castor oil (ECO), followed by carbonated castor oil (CCO), and ultimately

to the formation of the non-isocyanate poly (urethane amic acid) (NIPUAA) polymer. In the ^{1}H-NMR spectrum of ECO [Fig. 2(II)], the successful epoxidation of carbon–carbon double bonds in ricinoleate chains was evidenced by the appearance of characteristic proton signals of the oxirane (epoxy) ring near δ 3.2 ppm and the disappearance of doublet peaks around 5.5–6.0 ppm corresponding to the double bonds, as shown in Fig. 2(I). The 3.2 ppm signal corresponds to the methine and methylene protons adjacent to the epoxide ring, confirming the conversion of olefinic double bonds into epoxide functionalities.[18] The epoxy proton signal completely vanishes at about 3.2 ppm in the CCO spectrum [Fig. 2(III)] after the carbonation of ECO *via* CO_2, signifying that the cycloaddition reaction between CO_2 and the epoxide rings was successful in producing the required amount of carbonated castor oil (CCO). It is replaced by new multiplet signals in the δ 4.3–4.9 ppm range [Fig. 2(III)], which are caused by methine and methylene protons on the five-membered cyclic carbonate rings.[19] Noticeable spectral changes are observed in the ^{1}H-NMR spectrum after the final polycondensation between CCO, IPDA and PMDA, leading to the formation of NIPUAA [Fig. 2(IV)]. The polymerization step is marked by the presence of broad signals in the region around 8.5–9.0 ppm, corresponding to the urethane bond in the polymer backbone. In addition, the successful incorporation of PMDA is evidenced by the appearance of a distinct multiplet corresponding to aromatic proton in the δ 7.14–7.17 ppm range, thereby confirming the incorporation of pyromellitic units in the polymer backbone.

3.1.2 FTIR spectroscopy. The successful conversion of the C=C bonds in castor oil (CO) to epoxy groups in epoxidized castor oil (ECO) was confirmed by FT-IR spectroscopy, as illustrated in Fig. 3. In the FTIR spectrum of CO [Fig. 3(I)], a characteristic absorption band near 3000 cm^{-1} corresponds to the stretching vibration of unsaturated =C–H bonds. This peak completely disappears in the ECO spectrum [Fig. 3(II)], indicating the consumption of double bonds during the epoxidation process. Furthermore, the olefinic C=C stretching band observed at approximately 1648 cm^{-1} in CO also vanishes in ECO, providing additional evidence for the successful epoxidation reaction. Most importantly, the formation of the epoxy functional group is confirmed by the appearance of two distinct absorption bands (a doublet) in the range of 830–850 cm^{-1}, which are assigned to the asymmetric and symmetric ring deformation vibrations of the oxirane (epoxy) ring.[18] Following this, the epoxy groups were further transformed into five-membered cyclic carbonate structures *via* carbonation with CO_2, and this transformation is evident from the disappearance of the epoxy ring peaks (around 830–850 cm^{-1}) in the CCO spectrum [Fig. 3(III)]. Simultaneously, new absorption bands emerge in the region of 1790–1805 cm^{-1}, which are attributed to the C=O stretching of cyclic carbonate groups [Fig. 3(III)]. These observations confirm the efficient ring-opening carbonation of epoxide groups into cyclic carbonates.[19] Subsequently, the ring-opening polyaddition of the cyclic carbonate with IPDA, followed by the incorporation of PMDA, leads to the formation of non-isocyanate poly (urethane amic acid) (NIPUAA). FTIR analysis of the final NIPUAA polymer [Fig. 3(IV)] provides clear evidence of the successful structural transformation. The disappearance of the characteristic cyclic carbonate C=O stretching band around 1790 cm^{-1} indicates the complete consumption of cyclic carbonate groups during the aminolysis reaction. New absorption bands emerge in the region of 3320–3360 cm^{-1}, assigned to N–H stretching vibrations, and 1680–1720 cm^{-1}, corresponding to the C=O stretching of the urethane bond, confirming the formation of urethane linkages in the polymer backbone.[20] Additionally, the characteristic symmetric and asymmetric stretching vibrations of the dianhydride moiety, typically observed around 1850 cm^{-1} and 1780 cm^{-1}, are absent in the final FTIR spectrum of NIPUAA. This disappearance confirms the complete ring opening of the dianhydride units and their successful incorporation as amic acid linkages (C=O stretching band at 1630 cm^{-1}) in the polymer network.[21] Together, these spectral features validate the efficient isocyanate-free synthesis route and the covalent integration of both carbonate and dianhydride components into the final NIPUAA structure. The FTIR spectra of NIPUAA-132 and NIPUAA-143 are provided in Fig. S1 and S2, which depict peaks similar to those of NIPUAA-121.

3.2 Thermal properties

3.2.1 Thermogravimetric analysis (TGA). The thermal stability and degradation behaviour of the synthesized non-isocyanate poly (urethane amic acid) (NIPUAA) coatings were evaluated by thermogravimetric analysis (TGA) over a temperature range of 30–800 °C under a nitrogen atmosphere at a constant heating rate of 10 °C min^{-1}. The TGA thermograms [shown in Fig. 4(a) and (b)] demonstrated a three-step degradation profile, showing the influence of the segmented NIPUAA chemical structure and molecular composition on the thermal decomposition mechanism. The breakdown of urethane linkages and potential partial dissociation of amic acid moieties introduced during the step-growth polyaddition between IPDA and PMDA are responsible for the first weight loss (1st T_d),[22] which occurs roughly in the temperature range of 170–240 °C. At all stages of thermal deterioration, NIPUs continuously release CO_2, but the emission noticeably decreases at higher temperatures. NIPUs show a more noticeable CO_2 evolution than traditional polyurethanes because of their increased density of urethane links. The primary degradation products of these urethane groups are ammonia and carbon dioxide, making early-stage gas evolution a useful indicator of initial thermal stability. Interestingly, the degradation pathways of both PU and NIPUAA follow a similar trajectory initiated by urethane bond cleavage that yields CO_2 and polyols.[23] From Table 1, it is seen that the NIPUAA-121 composition had the highest first degradation temperature (T_{d_1}) of the three compositions, around 230 °C. This suggests that the composition was slightly more thermally stable during its initial degradation phase, most likely because it contained fewer rigid hard segments. As the amount of IPDA and PMDA increased, however, NIPUAA-132 and NIPUAA-143 showed T_{d_1} values of 182 °C and 177 °C, respectively. This trend can be attributed to the increasing concentration of urethane groups with

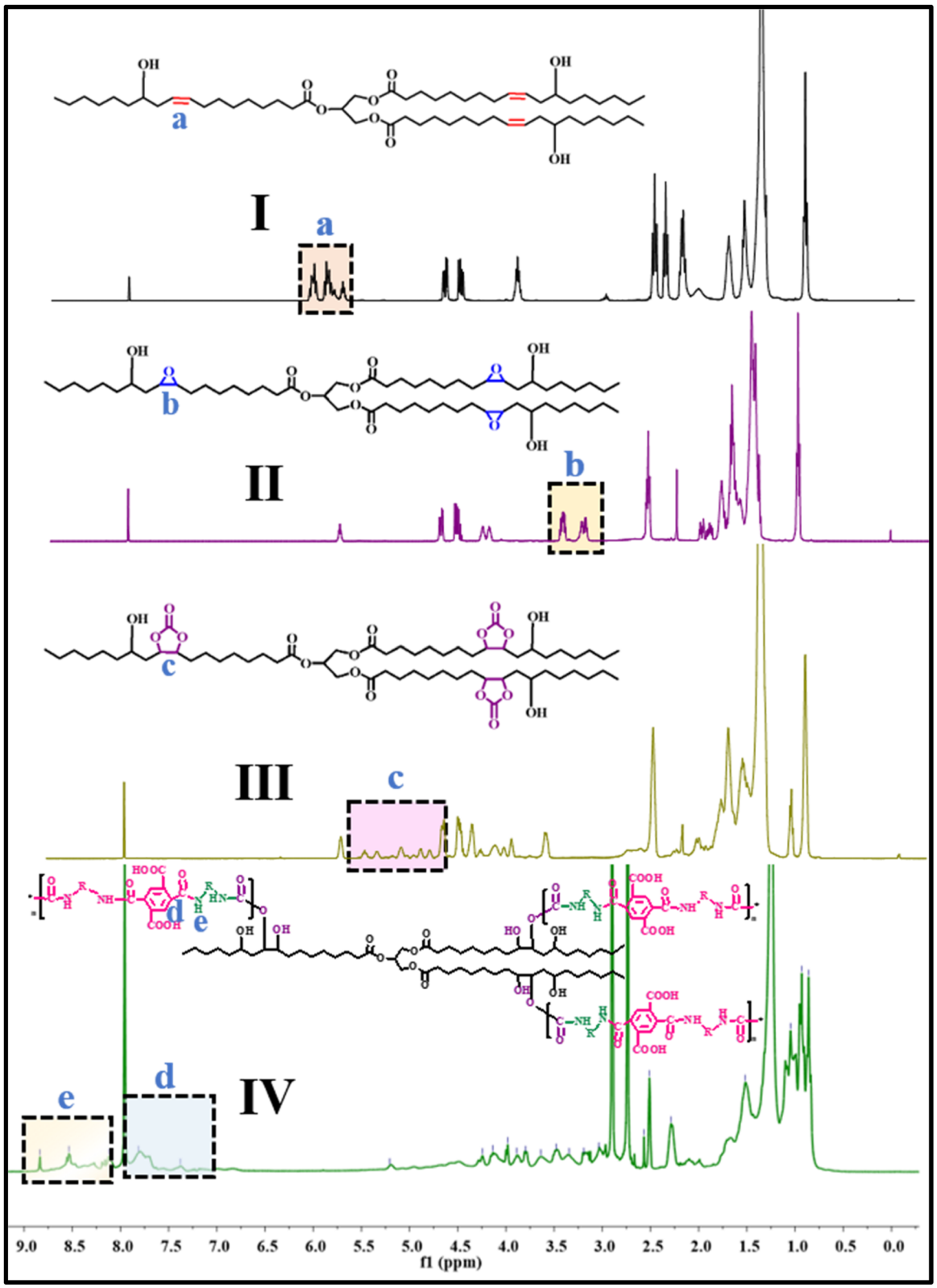

Fig. 2 ^{1}H-NMR spectra of (I) CO, (II) ECO, (III) CCO and (IV) the NIPUAA coating.

increasing IPDA and PMDA content since urethane groups are very labile. The breakdown of long aliphatic chains derived from the soft segment part of NIPUAA, which corresponds to the carbonated castor oil (CCO) (soft segment), is responsible for the second weight loss (T_{d_2}), which was observed in the temperature range of 400–440 °C. This mass loss corresponds to

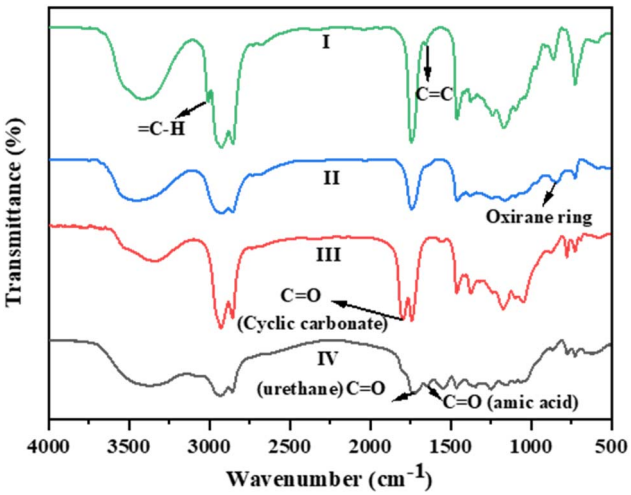

Fig. 3 FT-IR spectra of (I) CO, (II) ECO, (III) CCO and (IV) the NIPUAA coating.

β-scission of fatty acid esters, ester pyrolysis, and oxidative fragmentation of the hydrocarbon matrix, which are characteristic of triglyceride-based polyols derived from vegetable oils. The narrow range of degradation temperatures across all formulations indicates uniform integration of the soft segment backbone, confirming consistent structuring of CCO-derived oligomers within the NIPUAA polymer matrices.[23,24] The cleavage of C–C and C–O bonds within the aromatic and urethane-rich hard segment backbones is linked to the final degradation stage, which was observed in the temperature range of 450–500 °C. This is reflected in the thermal degradation pattern of NIPUAA-143, where the third degradation step begins around 499 °C, due to thermally resilient amic acid units backed up by a higher concentration of aromatic groups in PMDA.[24] NIPUAA-121 and NIPUAA-132 exhibited lower T_{d_3} values of 452 °C and 494 °C, respectively, due to the relatively fewer aromatic and amic acid moieties.

3.2.2 Differential scanning calorimetry (DSC) analysis. The DSC thermograms, [as shown in Fig. 4(c) and (d)], were recorded in a nitrogen atmosphere at temperatures ranging from −50 °C to 300 °C. The DSC curves of all three NIPUAA formulations showed a single, distinct T_g corresponding to the hard segment of the polymer since all the formulations contain castor oil as the soft segment, which typically shows a T_g around −55 °C.[25] In NIPUAA-121, a T_g of 17.14 °C and a T_m of 184.28 °C were observed. Increasing the proportion of IPDA and PMDA in NIPUAA-132 led to a slightly reduced T_g (14.70 °C) but an elevated T_m (205.40 °C), suggesting the formation of more crystalline hard segment microdomains leading to phase separation, which in turn leads to a decrease in the soft segment T_g and an increase in the hard segment T_g and/or melting point. Further, NIPUAA-143, which had the highest concentration of hard segments, showed a notable rise in T_g to 36.04 °C, indicating the influence of the increased H-bonding density and rigid aromatic content of the polymer network contributed by the incorporation of pyromellitic dianhydride (PMDA). Aromatic hard segments are known to significantly increase T_g due to their rigidity and strong π–π interactions, which reduce chain mobility and enhance thermal dimensional stability. These effects are widely attributed to the presence of stiff aromatic rings, which form tightly packed domains capable of π–π stacking and extensive hydrogen bonding. As the hard-segment content increases, the resulting rigidity and cohesive energy density significantly hinder chain mobility, thereby raising T_g.[26] Such thermal performance is particularly desirable for protective coatings on metal substrates, where exposure to elevated temperatures, UV radiation, and corrosive environments can severely impact the integrity of coatings. The production of defective crystalline areas or higher steric hindrance from excess hard segments may be the cause of the modest decrease in T_m (180.17 °C) when compared to NIPUAA-132. The observed trends show that the segmental dynamics and thermal stability of NIPUAA coatings are altered when the hard-segment content (IPDA and PMDA) is increased. While T_m represents the growth of crystalline domains influenced by chain regularity and packing efficiency, T_g increases with hydrogen-bonding density and aromatic rigidity. Thus, the balance between flexible aliphatic polyols and rigid aromatic structures governs both T_g and thermal degradation thresholds. The absence of cold crystallization exotherms and the presence of distinct melting transitions further support the semi-crystalline or phase-locked amorphous nature of the systems, stabilized by intermolecular interactions among urethane, urea, and amic acid functionalities.[27]

3.3 Coating properties on mild steel substrates

3.3.1 Adhesion strength. The adhesion performance of the synthesized non-isocyanate poly (urethane amic acid) (NIPUAA) coatings on mild steel substrates was evaluated and found to be around 0.53 MPa, 0.65 MPa, and 0.68 MPa for NIPUAA-121, NIPUAA-132, and NIPUAA-143 formulations, respectively [Table 2]. These values demonstrate a consistent improvement in adhesion with increasing hard segment content, reflecting enhanced interfacial bonding properties. The moderate yet promising adhesion strength may be attributed to multiple molecular-level interactions occurring at the coating-substrate interface. Specifically, the urethane and amic acid functionalities within the polymer network are capable of forming hydrogen bonds and coordinate interactions with the hydroxylated and oxide-rich surface of mild steel. The amic acid groups present in the backbone may also contribute to secondary hydrogen bonding at the interface, subtly improving the cohesive strength of the coating film.[28,29] In addition, the polar groups introduced through the pyromellitic dianhydride (PMDA) moiety enhance the surface energy of the NIPUAA matrix, improving its wettability and mechanical anchoring on the metallic substrate. The gradual increase in adhesion strength from NIPUAA-121 to NIPUAA-143 may also be related to the higher density of reactive polar groups and the increased rigidity of the matrix, which collectively promote closer contact and reduced interfacial voids.[30] Moreover, the isocyanate-free approach to synthesis removes a common source of undesirable side reactions with surface moisture, which can adversely

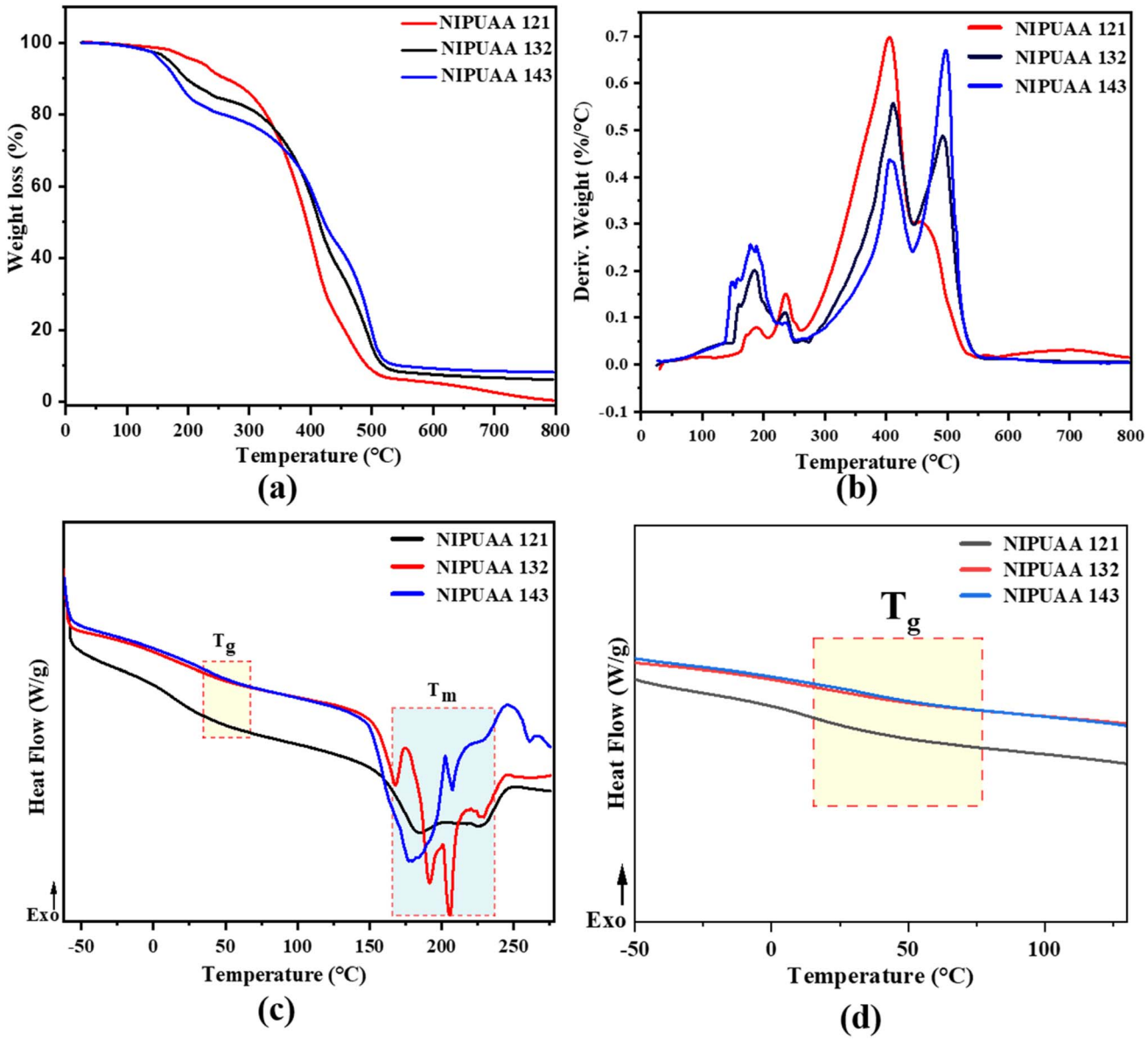

Fig. 4 (a) Weight loss (%) curves; (b) derivative weight (%/°C) curves; (c) DSC curves; (d) zoomed T_g curves of the DSC analysis of the NIPUAA-121, NIPUAA-132 and NIPUAA-143 films.

Table 1 Thermal properties of NIPUAA coatings

	Degradation temperature ($T_{d_{max}}$) (TGA)				Thermal transitions (DSC)	
Sample code	T_{d_1} (°C)	T_{d_2} (°C)	T_{d_3} (°C)	Residual mass at 790 °C (%) (TGA)	T_g (°C)	T_m (°C)
NIPUAA-121	233.3	406.2	452.5	1.72	17.14	184.28
NIPUAA-132	182.4	410.5	494.5	2.11	14.70	205.40
NIPUAA-143	177.1	408.4	499.6	1.40	36.04	180.17

affect the coating adhesion. In conventional isocyanate-based systems, any water present can react with free –NCO groups, producing CO_2 gas and urea byproducts, resulting in blisters, pinholes, and delamination that compromise adhesion and coating integrity.[31]

3.3.2 Abrasion resistance. A crucial metric for coating endurance is the wear and tear index, which is measured in milligrams of mass loss per 1000 cycles per kilogram. All formulations showed a noticeably low wear rate, as shown in Table 2. Specifically, NIPUAA-143 exhibited the lowest mass loss

Table 2 Coating properties of NIPUAA

Test/sample	NIPUAA-121	NIPUAA-132	NIPUAA-143
Adhesion pull off	0.53 MPa	0.65 MPa	0.68 MPa
Abrasion resistance	0.092 mg	0.119 mg	0.076 mg
Pencil hardness	H	2H	2H
Cone mandrel test	No cracking/peeling in the cone mandrel test	No cracking/peeling in the cone mandrel test	No cracking/peeling in the cone mandrel test
Salt spray analysis	120 h	120 h	120 h

of 76 mg per 1000 cycles, indicating superior wear resistance among the three compositions. NIPUAA-121 and NIPUAA-132 recorded 92 mg and 119 mg, respectively, suggesting moderate resistance to surface abrasion. Harder films resulting from higher amic acid content may be the reason for the superior performance of NIPUAA-143, which offers resistance to material loss under frictional stress. When compared with a few commercially available polymer systems[32] and some reported PU systems,[33] these NIPUAA coatings demonstrate equal or slightly superior abrasion resistance. These comparisons highlight that the castor oil-based NIPUAAs presented here, despite their simplified formulation and absence of reinforcing fillers or post-synthetic cross-linking, already meet or exceed the abrasion tolerance of related systems. This level of performance can be attributed to the balanced molecular architecture of the NIPUAA networks. The urethane and amic acid linkages formed through the reaction of carbonated castor oil, isophorone diamine (IPDA), and pyromellitic dianhydride (PMDA) create a segmented structure, in which rigid aromatic domains are interspersed within flexible aliphatic chains. The incorporation of pyromellitic-based hard segments introduces aromatic rigidity, which enhances surface hardness and resistance to mechanical deformation, while the flexible aliphatic backbone of carbonated castor oil ensures toughness and resilience under cyclic wear. Furthermore, the presence of multiple hydrogen-bonding motifs arising from urethane, urea, and amic acid functionalities likely contributes to cohesive energy density at the molecular level, helping maintain the structural integrity of the coating under dynamic stress as discussed earlier in the TGA analysis. The absence of isocyanates in the synthesis process plays an additional role in enhancing long-term mechanical performance. Conventional isocyanate-based polyurethanes are prone to side reactions with ambient moisture during application and curing, leading to microvoids or local network defects that reduce adhesion and wear resistance. In contrast, the non-isocyanate route adopted here avoids such complications, resulting in a more uniform and defect-free film morphology that supports both adhesion and abrasion resistance.

3.3.3 Pencil hardness. This test is a qualitative measure of a coating's resistance to surface deformation and scratching. The NIPUAA coatings exhibited a pencil hardness rating of 2H, indicating that they can withstand penetration and scratching from a pencil with moderate hardness. This level of hardness reflects the structural characteristics of the coating matrix, particularly the balance between flexible aliphatic segments derived from CCO and the rigid, hydrogen-bonded hard segments introduced by PMDA and IPDA. The 2H hardness suggests that while the coating offers an appreciable level of surface durability suitable for general protective applications, it may be susceptible to damage under high mechanical stress or in environments requiring superior scratch resistance.[34] The moderate hardness can be correlated with the semi-crystalline to amorphous nature of the polymer films, as indicated by DSC results, which point to glass transition temperatures in the range of 14–36 °C and melting transitions above 180 °C. These thermal properties align with a coating system that is not overly brittle but still maintains sufficient cohesion to resist mild mechanical damage. The urethane and amic acid functionalities are known to form extensive H-bonding networks that contribute to cohesive energy density and surface integrity. However, the relatively high content of soft segments from castor oil derivatives imparts flexibility, which can somewhat compromise surface hardness while benefiting toughness and film-forming properties.

According to Lai *et al.*, a 2H hardness was attained by adding a more self-crosslinking ketone-hydrazide structure, which also greatly increased the tensile strength of the film and decreased its water absorption.[35] As a result, the 2H pencil hardness found in our bio-based, isocyanate-free NIPUAA coatings is especially promising because it offers increased sustainability and environmental advantages along with comparable mechanical robustness.

3.3.4 Cone mandrel test. This test provides a practical measure of the ability of coatings to withstand mechanical deformation, particularly bending and elongation, without failure. The NIPUAA-coated mild steel panels were subjected to progressive bending to 180° over a conical mandrel and remarkably, all tested NIPUAA-121, NIPUAA-132, and NIPUAA-143 coatings exhibited outstanding flexibility, with no visible signs of cracking, delamination, or surface rupture throughout the test. The soft segment (CCO) contributes significantly to chain mobility and ductility. The aliphatic, triglyceride-derived backbones from castor oil provide long, flexible chains that can accommodate strain without leading to structural failure.[36] Meanwhile, the hard segments derived from PMDA and IPDA serve to maintain film integrity through strong intermolecular interactions, such as H-bonding, between urethane and amic acid groups as discussed earlier. The absence of microcracking even under severe bending conditions indicates a well-balanced phase-separated morphology, where soft domains facilitate flexibility while hard domains provide mechanical strength and adhesion. Conventional polyurethane coatings synthesized *via*

isocyanate routes often suffer from molecular embrittlement when exposed to ambient moisture that triggers side reactions, such as the formation of urea, biuret, and allophanate linkages, leading to increased cross-link density and reduced flexibility in the cured film.[37] However, the isocyanate-free pathway used here ensures a more stable polymer backbone. This synthetic advantage is further manifested in the flexibility observed, making NIPUAA coatings particularly attractive for dynamic applications where coatings must endure repeated mechanical deformation.

3.4 Anticorrosion studies

3.4.1 Tafel polarization studies. The Tafel polarization characterization evaluates the performance of coatings against the corrosion of mild steel in a 3.5% NaCl solution (Fig. 5). This data, compiled in Table 3, is an analysis of NIPUAA coating performance, which includes the initial day of the mild steel panel and after three days of immersion in 3.5% NaCl. From the Tafel analysis, the key findings are corrosion potential (E_{corr}), corrosion current density (i_{corr}), corrosion rate, and polarization resistance (R_p), which are crucial parameters to measure the efficacy of these coatings. The $E_{corr,}$ which represents the equilibrium potential at which anodic and cathodic reactions balance, should be positive for well-performing or negative for low-efficiency coatings. The data from Table 3 shows that MS exhibits the most negative E_{corr} at −616 mV, indicating its high corrosion tendency. In contrast, before exposure to NaCl, the NIPUAA coatings demonstrated lower or less negative E_{corr} values, indicating superior initial corrosion resistance. However, after 3 days of exposure of these coated MS panels to 3.5% NaCl, all coatings exhibit a significant negative shift in E_{corr}, highlighting an increase in corrosion. Another important parameter from this study is corrosion current density (i_{corr}), which is directly proportional to the corrosion rate. Before NaCl exposure, NIPUAA-132 shows the lowest i_{corr} (0.256×10^{-3} nA), suggesting superior corrosion resistance, whereas mild steel exhibits a significantly higher i_{corr} (6.04 nA), confirming its susceptibility to corrosion. After immersion for three days, i_{corr} increases for all samples, demonstrating an increasing corrosion rate and current density.[38–41]

With the lowest corrosion rate (2.97×10^{-6} mm per year), NIPUAA-132 highlights its exceptional corrosion resistance. The corrosion rates of all samples, however, increase after three days

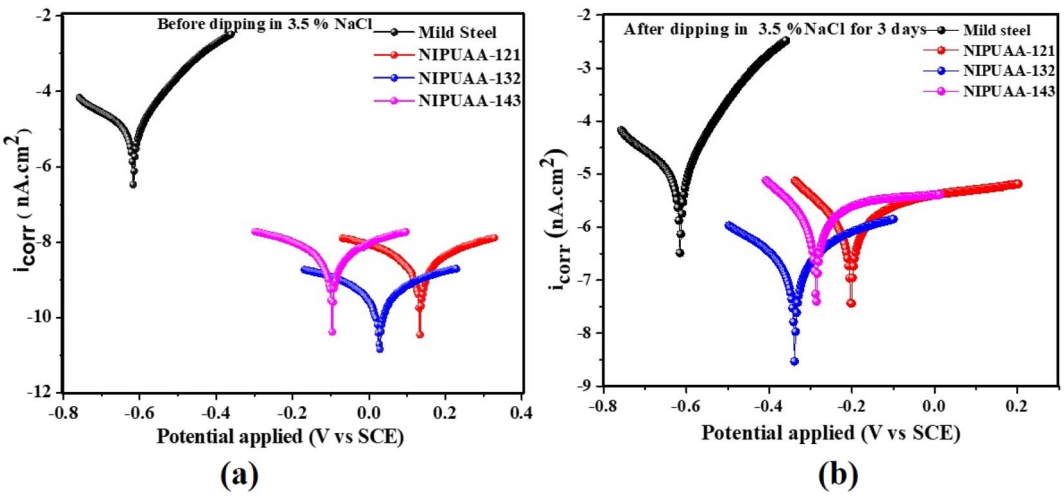

Fig. 5 (a)Tafel plots for the mild steel, NIPUAA-121, NIPUAA-132 and NIPUAA-143 before dipping in 3.5% NaCl solution. (b) Tafel plots for the mild steel, NIPUAA-121, NIPUAA-132, and NIPUAA-143 after dipping in a 3.5% NaCl solution.

Table 3 Tafel polarization data of NIPUAA coatings

System	E_{corr} (mV)	i_{corr} (nA)	Corrosion rate (mm per year)	Polarization resistance (MΩ)
Mild steel	−616	6.04	7.02×10^{-2}	2.94×10^{-3}
Before dipping in 3.5% NaCl				
NIPUAA-121	134.64	1.85	2.15×10^{-5}	22
NIPUAA-132	29.17	0.256×10^{-3}	2.97×10^{-6}	148.64
NIPUAA-143	−95.22	1.78	2.07×10^{-5}	14.35
After dipping in 3.5% NaCl for 3 days				
NIPUAA-121	−202.01	372.2	4.32×10^{-3}	45.33×10^{-3}
NIPUAA-132	−338.37	112.62	1.3×10^{-3}	250.5×10^{-3}
NIPUAA-143	−286.51	514.05	5.97×10^{-3}	35.76×10^{-3}

in NaCl; in contrast, NIPUAA-143 has the highest corrosion rate (5.97×10^{-3} mm per year), indicating that it performs worse in extended saline conditions. The greatest R_p (148.64 MΩ) is displayed by NIPUAA-132, confirming its superior anti-corrosion capabilities. All samples, however, show a decrease in R_p following three days in NaCl. Despite this, NIPUAA-132 continues to exhibit the greatest post-exposure R_p (250.5×10^{-3} MΩ), indicating that it performs better over the long term than the other NIPUAA coatings. In conclusion, because of its lowest corrosion rate, lowest i_{corr} values, and maximum polarization resistance, NIPUAA-132 is the most effective. To improve long-term durability in harsh conditions, more material optimization is necessary, as prolonged exposure to 3.5% NaCl reduces protective performance. By replacing conventional isocyanate coatings with non-isocyanate PU coatings, this investigation offers important insights into protective coatings, with fewer adverse effects on the environment or human health.[41] A comparative table [Table S5] has been prepared to compare the anticorrosion data with previously reported literature, where we could see that NIPUAA coatings offer promising results towards sustainable, isocyanate-free anticorrosive coatings.

Table 4 EIS characterization data of NIPUAA coatings

NIPUAA system	EIS (R_{ct}, MΩ)	Bode modulus (Ω cm^{-2})	Bode phase (θ)
Mild steel	131×10^{-6}	20.62	2.07
NIPUAA-121	9.68	9.7×10^{-3}	84.8
NIPUAA-132	82.2	9.4×10^{-3}	86.41
NIPUAA-143	8.4	8.6×10^{-3}	66.43

3.4.2 Electrochemical impedance spectroscopy (EIS). The electrochemical impedance of the coatings was studied using steady-state open circuit potential (OCP) measurements in a 3.5% NaCl solution (Table 4). The Nyquist plots exhibited semi-circular patterns that were effectively fitted using a Randles circuit, comprising R_s (solution resistance), R_{ct} (charge transfer resistance), and a constant phase element (CPE) with its modulus represented by Y_0. Higher R_{ct} values indicate enhanced resistance to charge transfer at the interface between the steel panel and corrosion environment.[42] All coated samples underwent EIS testing, followed by immersion in the saline medium for 48 hours for NIPUAA-121 and NIPUAA-132, and 72 hours for NIPUAA-143, as shown in Fig. 6. NIPUAA-132 displayed excellent charge transfer resistance among the formulated specimens (NIPUAA-121 and 143), as shown in the Nyquist plot [Fig. 6(a)] with a significantly higher R_{ct} value of 82.2 MΩ. In conclusion, both Nyquist and Bode analyses [Fig. 6(b) and (c)] confirmed the superior protective capabilities of the NIPUAA-132 coating on mild steel.

3.4.3 Salt spray analysis. The salt spray fog test was conducted to assess the extent of damage propagation, including delamination and mechanical failure of the coating. Images of the coated panels were captured after up to 120 hours of exposure to a 5% (w/v) sodium chloride (NaCl) solution, as shown in Table S4. Fig. 7 depicts the salt spray exposure of the coated and

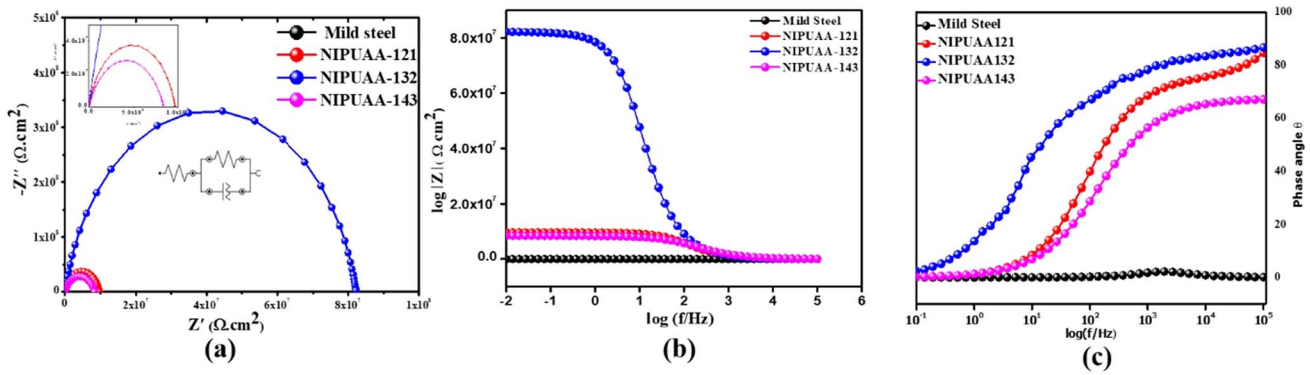

Fig. 6 (a) Nyquist plots of NIPUAA-121, NIPUAA-132 and NIPUAA-143, (b) Bode plots of NIPUAA-121, NIPUAA-132 and NIPUAA-143, and (c) Bode phase angle of NIPUAA coatings on steel panels. Data were obtained after 2–3 days of immersion in a 3.5% salt solution.

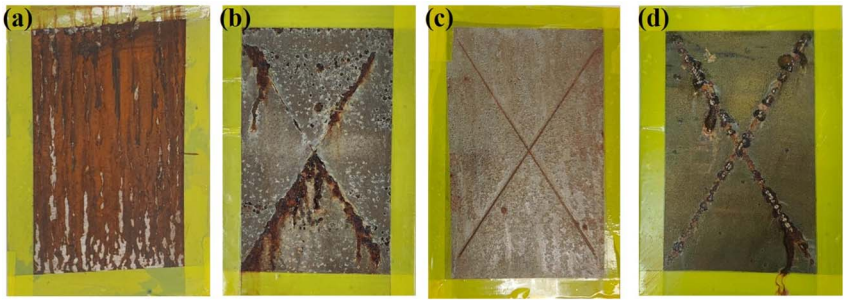

Fig. 7 Salt spray analysis of (a) bare uncoated mild steel panel, (b) NIPUAA-121, (c) NIPUAA-132 and (d) NIPUAA-143 after 120 h of exposure.

bare uncoated mild steel panel after 120 hours. The results revealed that the coating without NIPUAA, as shown in Fig. 7(a), exhibited early signs of delamination, indicating reduced adhesion and compromised protective performance.[43] In contrast, the NIPUAA-coated panels demonstrated superior adhesion strength and significantly enhanced corrosion resistance, highlighting the effectiveness of NIPUAA in improving the durability and protective properties of the coating under corrosive conditions.

4. Conclusion

The current study shows that castor oil, a commercially available non-edible oil, can be converted into high-performance poly (urethane amic acid) coatings suitable for shielding mild steel and galvanised iron sheets through an isocyanate-free process. FTIR, ^{1}H NMR, and elemental analysis verified the structures of the NIPUAA networks produced by step-wise epoxidation, carbonation, and subsequent polycondensation with isophorone diamine and pyromellitic dianhydride. TGA showed three-stage degradation with final onset temperatures near 500 °C, highlighting good thermal stability at service temperatures well above ambient. Thermal characterization showed single T_g values between 15 and 36 °C and melting transitions above 180 °C, indicating a balanced semi-crystalline morphology. Mechanical testing revealed that the films combine surface durability and flexibility: pencil hardness reached 2H, Taber abrasion losses averaged 92 mg/1000 cycles, and cone-mandrel bending resulted in neither cracking nor delamination. Strong interfacial hydrogen bonding between the urethane/amic functionalities and the oxide-rich steel surface is demonstrated by adhesion strengths of 0.53–0.68 MPa, which were obtained without primers. The formulation that consistently outperformed the others was NIPUAA-132, which was balanced at a CCO : IPDA : PMDA molar ratio of 1 : 3 : 2. It had the lowest initial corrosion current density (0.256×10^{-3} nA), the smallest corrosion rate (2.97×10^{-6} mm per year), the highest polarisation resistance (148.6 MΩ initial, 250 kΩ after 72 h), and the largest charge-transfer resistance (82.2 MΩ) in EIS. In sharp contrast, salt-spray photos taken 120 hours later showed very little blistering or under-film corrosion. All of these results support a sustainable, isocyanate-free route to coatings that meet or surpass a number of traditional polyurethane standards while eliminating hazardous precursors and lowering carbon emissions. Future improvements in abrasion and long-term weathering resistance, such as post-cure imidization, nanofiller reinforcement, or fine-tuning the hard-segment content, should enable bio-derived NIPUAAs to replace petrochemical polyurethanes in demanding anti-corrosion applications.

Author contributions

Rakesh Rapolu: data curation, methodology, formal analysis, validation, writing – original draft. Kashmiri Borah: data curation, methodology, formal analysis, validation, writing – original draft. P. Ermiya Prasad: data curation, formal analysis P. Aruna: conceptualization, investigation, supervision, writing – review and editing.

Conflicts of interest

There are no conflicts to declare.

Data availability

Data will be made available on request.

Supplementary information (SI): epoxy value estimation and additional data (PDF). See DOI: https://doi.org/10.1039/d5su00835b.

Acknowledgements

All the authors acknowledge the Director, IICT, for financial support under the IICT Research Grant (IRG, project code-MLP 9017, manuscript No. IICT/Pubs./2025/237). The authors also wish to acknowledge Mr L. Yugender Raju, Mr Sandeep Kumar, and Dr Anitha PM for their technical assistance during the investigation.

References

1 A. Pistone, C. Scolaro and A. Visco, A review on Mechanical properties of protective coatings against marine fouling, *Polymers*, 2021, **13**, 173, DOI: 10.3390/polym13020173.
2 R. Kanchana, M. Ponnuchamy, A. Kapoor and P. B. Sethupathi, Coatings in the Automobile Application in: Functional Coatings for Biomedical, *Energy, and Environmental Applications*, John Wiley & Sons, Inc., 1st edn, 2024, pp. 343–361. DOI: 10.1002/9781394263172.ch15.
3 A. N. Obaid and E. Al-Bermany, Impact of graphene nanosheets on adhesion and corrosion performance of reinforced polyurethane coating for aerospace aluminium alloy T3, *Int. J. Adhes. Adhes.*, 2024, **132**, 103695, DOI: 10.1016/j.ijadhadh.2024.103695.
4 B. Shojaei, M. Najafi, A. Yazdanbakhsh, M. Abtahi and C. Zhang, A review on the applications of polyurea in the construction industry, *Polym. Adv. Technol.*, 2021, **32**, 2797–2812, DOI: 10.1002/pat.5277.
5 C. A. Krone, Diisocyanates and nonoccupational disease: a review, *Arch. Environ. Health*, 2003, **58**, 306–316, DOI: 10.3200/AEOH.58.6.306-316.
6 K. Nakashima, T. Takeshita and K. Morimoto, Review of the occupational exposure to isocyanates: mechanisms of action, *Environ. Health Prev. Med.*, 2002, **7**, 1–7, DOI: 10.1007/BF02898058.
7 *MDI and TDI: Safety, Health and the Environment: A Source Book and Practical Guide*, ed. D. C. Allport, D. S. Gilbert and S. M. Outterside, John Wiley & Sons, 2003.
8 A. Delavarde, G. Savin, P. Derkenne, M. Boursier, R. Morales-Cerrada, B. Nottelet, J. Pinaud and S. Caillol, Sustainable polyurethanes: toward new cutting-edge opportunities, *Prog. Polym. Sci.*, 2024, **151**, 101805, DOI: 10.1016/j.progpolymsci.2024.101805.

9 S. I. Bhat, M. Mobin, S. Islam and S. Zehra, Recent advances in anticorrosive coatings based on sustainable polymers: Challenges and perspectives, *Surf. Coat. Technol.*, 2024, **480**, 130596, DOI: 10.1016/j.surfcoat.2024.130596.
10 M. Rayung, N. Abd Ghani and N. Hasanudin, A review on vegetable oil-based non-isocyanate polyurethane: towards a greener and sustainable production route, *RSC Adv.*, 2024, **14**, 9273–9299, DOI: 10.1039/D3RA08684D.
11 A. Didenko, G. Vaganov, A. Nesterova, A. Kamalov, V. Lavrentiev, E. Popova, V. Kraft, T. Anokhina, I. Borisov, I. Abalov and K. Polotnyanshchikov, Porous nonwoven calendered fabrics (membranes) based on electrospun prepolymers of modified polyimides, *Polym. Eng. Sci.*, 2025, **65**, 1665–1681, DOI: 10.1002/pen.27071.
12 P. S. G. Krishnan, C. Z. Cheng, Y. S. Cheng and J. W. C. Cheng, Preparation of nanoporous polyimide films from poly(urethane-imide) by thermal treatment, Macromol, *Mater. Eng.*, 2003, **288**, 730–736, DOI: 10.1002/mame.200300030.
13 Y. Feng, L. Man, Y. Hu, L. Chen, B. Xie, C. Zhang, T. Yuan and Z. Yang, One-pot synthesis of polyurethane-imides with tailored performance from castor and tung oil, *Prog. Org. Coat.*, 2019, **132**, 62–69, DOI: 10.1016/j.porgcoat.2019.03.035.
14 Y. R. Sulthana, D. K. Chelike and S. A. G. Thangavelu, Biorenewable vegetable oil based nonisocyanate polyurethanes and nanocomposites; formulation, characterisation, biodegradation, anticorrosion and antifouling coatings, *New J. Chem.*, 2024, **48**, 5173–5185, DOI: 10.1039/D3NJ05862J.
15 J. Pouladi, S. M. Mirabedini, H. E. Mohammadloo and N. G. Rad, Synthesis of novel plant oil-based isocyanate-free urethane coatings and study of their anti-corrosion properties, *Eur. Polym. J.*, 2021, **153**, 110502, DOI: 10.1016/j.eurpolymj.2021.110502.
16 C. E. Chuka, B. O. Odio, J. L. Chukwuneke and J. E. Sinebe, Investigation of the effect of corrosion on mild steel in five different environments, *Int. J. Sci. Technol. Res.*, 2014, **3**, 306–310.
17 R. Bender, D. Féron, D. Mills, S. Ritter, R. Bäßler, D. Bettge, I. De Graeve, A. Dugstad, S. Grassini, T. Hack and M. Halama, Corrosion challenges towards a sustainable society, *Mater. Corros.*, 2022, **73**, 1730–1751, DOI: 10.1002/maco.202213140.
18 G. Thirupathiah, S. Satapathy and A. Palanisamy, Studies on epoxidised castor oil as co-plasticizer with epoxidised soyabean oil for PVC processing, *J. Renewable Mater.*, 2019, **7**, 775–785, DOI: 10.32604/jrm.2019.06399.
19 N. Dhore, A. O. Kottaron, A. Palanisamy and R. Narayan, Carbonated castor oil as a bioplasticiser and toughening agent for bisphenol A based epoxy, *J. Appl. Polym. Sci.*, 2024, **141**, e55828, DOI: 10.1002/app.55828.
20 N. Dhore, E. Prasad, R. Narayan, C. R. Rao and A. Palanisamy, Studies on biobased non-isocyanate polyurethane coatings with potential corrosion resistance, *Sustainable Chem.*, 2023, **4**, 95–109, DOI: 10.3390/suschem4010008.
21 H. Deligöz, T. Yalcınyuva and S. Özgümüs, A novel type of Si-containing poly(urethane-imide)s: synthesis, characterization and electrical properties, *Eur. Polym. J.*, 2005, **41**, 771–778, DOI: 10.1016/j.eurpolymj.2004.11.007.
22 S. Oprea, Effect of composition and hard-segment content on thermo-mechanical properties of cross-linked polyurethane copolymers, *High Perform. Polym.*, 2009, **21**, 353–370, DOI: 10.1177/0954008308092071.
23 A. Bukowczan, I. Łukaszewska and K. Pielichowski, Thermal degradation of non-isocyanate polyurethanes, *J. Therm. Anal. Calorim.*, 2024, **149**, 10885–10899, DOI: 10.1007/s10973-023-13177-y.
24 H. J. Kim, X. Jin and J. W. Choi, Investigation of bio-based rigid polyurethane foams synthesized with lignin and castor oil, *Sci. Rep.*, 2024, **14**, 13490, DOI: 10.1038/s41598-024-64318-8.
25 S. S. Kashyap, K. Borah, J. S. Shailesh Kumar, Z. Sheerazi, R. Narayan and M. Ahmed, Role of silicoaluminophosphate as a corrosion inhibiting nanocontainer and filler in environmentally benign bio-based hybrid coatings, *ACS Sustainable Resour. Manage.*, 2024, **1**, 1211–1224, DOI: 10.1021/acssusresmgt.4c00084.
26 M. Asensio, J. F. Ferrer, A. Nohales, M. Culebras and C. M. Gómez, The role of diisocyanate structure to modify properties of segmented polyurethanes, *Materials*, 2023, **16**, 1633, DOI: 10.3390/ma16041633.
27 D. Visser, H. Bakhshi, K. Rogg, E. Fuhrmann, F. Wieland, K. Schenke-Layland, W. Meyer and H. Hartmann, Green chemistry for biomimetic materials: Synthesis and electrospinning of high-molecular-weight polycarbonate-based nonisocyanate polyurethanes, *ACS Omega*, 2022, **7**, 39772–39781, DOI: 10.1021/acsomega.2c03731.
28 A. Gomez-Lopez, S. Panchireddy, B. Grignard, I. Calvo, C. Jerome, C. Detrembleur and H. Sardon, Poly(hydroxyurethane) adhesives and coatings: state-of-the-art and future directions, *ACS Sustain. Chem. Eng.*, 2021, **9**, 9541–9562, DOI: 10.1021/acssuschemeng.1c02558.
29 Q. Zhang, L. Yue, R. Yan, D. J. Liaw, J. Shi, Z. Li, C. Liang, Y. Cheng, Z. Ge and Y. Zhang, Highly tough and reliable poly(amic acid) with ballistic impact-resistance through modulation of hydrogen bonding interactions, *Macromol. Rapid Commun.*, 2023, **44**, 2300092, DOI: 10.1002/marc.202300092.
30 Y. Chen, J. Hu, X. Wu, S. Duan, H. Wang and T. Ma, Synthesis and evaluation of polyurethane as waterproof adhesion layer for steel bridge deck, *Polymers*, 2024, **16**, 3140, DOI: 10.3390/polym16223140.
31 A. L. D. da Silva, J. M. Martín-Martínez and J. C. M. Bordado, Influence of the free isocyanate content in the adhesive properties of reactive trifunctional polyether urethane quasi-prepolymers, *Int. J. Adhes. Adhes.*, 2006, **26**, 355–362, DOI: 10.1016/j.ijadhadh.2005.06.001.
32 V. Pejaković, R. Jisa and F. Franek, Abrasion resistance of selected commercially available polymer materials, *Tribol. Finn. J. Tribol.*, 2015, **33**, 21–27. Retrieved from https://journal.fi/tribologia/article/view/69241.

33 K. Kwiatkowski and M. Nachman, The abrasive wear resistance of the segmented linear polyurethane elastomers based on a variety of polyols as soft segments, *Polymers*, 2017, **9**, 705, DOI: 10.3390/polym9120705.

34 N. Sun, S. Wang, P. Wu, H. Zhu, J. Li, M. Liu, G. Feng, W. Li, M. Li, G. Lai and X. Yang, UV-curable optical silicone-modified materials with fairly high tensile strength, pencil hardness, and good thermal stability from 2-amantadine functionalized non-isocyanate polyurethane, Macromol, *Chem. Phys.*, 2025, **226**, e00192, DOI: 10.1002/macp.202500192.

35 X. Lai, Y. Shen and L. Wang, Preparation and properties of self-crosslinkable polyurethane/silane hybrid emulsion, *J. Polym. Res.*, 2011, **18**, 2425–2433, DOI: 10.1007/s10965-011-9656-9.

36 P. M. Paraskar, M. S. Prabhudesai and R. D. Kulkarni, Synthesis and characterizations of air-cured polyurethane coatings from vegetable oils and itaconic acid, *React. Funct. Polym.*, 2020, **156**, 104734, DOI: 10.1016/j.reactfunctpolym.2020.104734.

37 D. K. Chattopadhyay and K. V. S. N. Raju, Structural engineering of polyurethane coatings for high performance applications, *Prog. Polym. Sci.*, 2007, **32**, 352–418, DOI: 10.1016/j.progpolymsci.2006.05.003.

38 A. Bouoidina, E. Ech-chihbi, F. El-Hajjaji, B. El Ibrahimi, S. Kaya and M. Taleb, Anisole derivatives as sustainable-green inhibitors for mild steel corrosion in 1 M HCl: DFT and molecular dynamic simulations approach, *J. Mol. Liq.*, 2021, **324**, 115088, DOI: 10.1016/j.molliq.2020.115088.

39 Y. Ma, Y. Ye, H. Wan, L. Chen, H. Zhou and J. Chen, Chemical modification of graphene oxide to reinforce the corrosion protection performance of UV-curable polyurethane acrylate coating, *Prog. Org. Coat.*, 2020, **141**, 105547, DOI: 10.1016/j.porgcoat.2020.105547.

40 C. Xing, Z. Zhang, L. Yu, L. Zhang and G. A. Bowmaker, Electrochemical corrosion behaviour of carbon steel coated by polyaniline copolymers micro/nanostructures, *RSC Adv.*, 2014, **4**, 32718–32725, DOI: 10.1039/C4RA05826G.

41 Y. Dong, J. Liang, G. Liu, W. Ni and L. Shen, Preparation and anticorrosive property of soluble aniline tetramer, *Coatings*, 2019, **9**, 399, DOI: 10.3390/coatings9060399.

42 P. E. Prasad, K. Borah, A. Palanisamy and C. R. Rao, Electroactive additives into polyurethanes for high corrosion resistance coatings for mild steel, *Polym. Adv. Technol.*, 2024, **35**, e6502, DOI: 10.1002/pat.6502.

43 G. Cai, H. Wang, D. Jiang and Z. Dong, Degradation of fluorinated polyurethane coating under UVA and salt spray. Part I: Corrosion resistance and morphology, *Prog. Org. Coat.*, 2018, **123**, 337–349, DOI: 10.1016/j.porgcoat.2018.07.025.